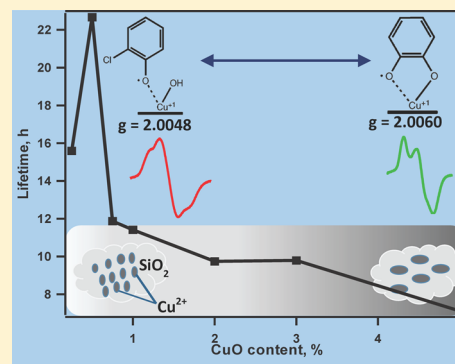


# Effect of Copper Oxide Concentration on the Formation and Persistency of Environmentally Persistent Free Radicals (EPFRs) in Particulates

Lucy W. Kiruri, Lavrent Khachatryan, Barry Dellinger, and Slawo Lomnicki\*

Department of Chemistry and LSU Superfund Research Center, Louisiana State University, Baton Rouge, Louisiana United States of America

**ABSTRACT:** Environmentally persistent free radicals (EPFRs) are formed by the chemisorption of substituted aromatics on metal oxide surfaces in both combustion sources and superfund sites. The current study reports the dependency of EPFR yields and their persistency on metal loading in particles (0.25, 0.5, 0.75, 1, 2, and 5% CuO/silica). The EPFRs were generated through exposure of particles to three adsorbate vapors at 230 °C: phenol, 2-monochlorophenol (2-MCP), and dichlorobenzene (DCBz). Adsorption resulted in the formation of surface-bound phenoxyl- and semiquinone-type radicals with characteristic EPR spectra displaying a *g* value ranging from ~2.0037 to 2.006. The highest EPFR yield was observed for CuO concentrations between 1 and 3% in relation to MCP and phenol adsorption. However, radical density, which is expressed as the number of radicals per copper atom, was highest at 0.75–1% CuO loading. For 1,2-dichlorobenzene adsorption, radical concentration increased linearly with decreasing copper content. At the same time, a qualitative change in the radicals formed was observed—from semiquinone to chlorophenoxyl radicals. The two longest lifetimes, 25 and 23 h, were observed for phenoxyl-type radicals on 0.5% CuO and chlorophenoxyl-type radicals on 0.75% CuO, respectively.



## INTRODUCTION

There is overwhelming evidence from animal experimental models, cell culture experiments, and cell free systems that exposure to particulate matter (PM) causes oxidative stress (OS)<sup>1,2</sup> leading to acute and chronic diseases.<sup>3–6</sup> OS results from excessive generation of reactive oxygen species (ROS) such as hydroxyl and superoxide radicals<sup>7,8</sup> under physiological conditions. Although a plethora of studies exist on the mortality and morbidity of PM, the components that are responsible for its toxicity and the observed adverse effects remain a quagmire.<sup>9–11</sup> However, many researchers agree that the level of PM toxicity depends on the chemical composition,<sup>12</sup> particle size,<sup>13</sup> and shape.<sup>14,15</sup> Recently, we reported that the presence of EPFRs on particulate matter reduces molecular O<sub>2</sub> to superoxide followed by dismutation in aprotic media to form hydrogen peroxide and hydroxyl radicals.<sup>16,17</sup> EPFRs on PM are formed through interaction of transition metal oxides (such iron, copper, zinc, and nickel) with aromatic compounds via surface mediated processes.<sup>18–21</sup> This results in the formation of surface-bound radical species which are stable enough to persist in the atmospheric environment for days, and which are also reactive in aquatic media to produce ROS.

The concentration of metals in particulate matter may vary greatly. In fine particulate matter (aerodynamic diameter <2.5 μm, PM<sub>2.5</sub>), 1–5 × 10<sup>3</sup>, 0.1–0.3, ~2.0, and 0.5–20 × 10<sup>3</sup> μg/g of Fe, Ni, Cu, and Zn, respectively, have been reported.<sup>22–25</sup> The analysis and characterization of transition metals from combustion systems and municipal incinerators reveals 2.35%

iron(III) oxide and 0.05% copper oxide.<sup>26,27</sup> Previous studies of EPFRs that used the same concentration of metals (5% by weight as oxide) in particulates indicated that almost every transition metal that was under study yielded EPFRs on particle surfaces.<sup>28–31</sup> The large distribution of metal concentration in particulate matter raises the question of how the metal concentration affects yield, lifetime, and chemical reactivity of the EPFRs. One can anticipate that changing the concentration of metal in particulates will affect the metal oxide cluster size and its reactivity. In fact, the size of metal/metal oxide clusters has been reported to be a pivotal property in the catalytic activity.<sup>32–37</sup> Changing catalytic properties may affect the propensity of the metal oxides to form EPFRs, hence contributing to the different chemical behavior of EPFRs. In this study, we are attempting to answer the above question by using different concentrations of copper oxide nanoclusters. Silica (Cabosil) based synthetic particulates containing varying concentrations of CuO (0.25–5% by weight) were tested for EPFRs' yield and persistence.

## EXPERIMENTAL SECTION

**Particle Synthesis.** Cabosil from Cabot (EH-5, 99+%, 88 m<sup>2</sup>/g BET surface area) was impregnated with a 0.1 M solution

Received: September 9, 2013

Revised: December 4, 2013

Accepted: January 17, 2014

Published: January 17, 2014

of  $\text{Cu}(\text{NO}_3)_2 \cdot 2.5\text{H}_2\text{O}$  to obtain particles with different copper oxide concentrations: 0.25, 0.5, 0.75, 1, 2, 3, and 5 wt %. Samples were left to adsorb copper nitrate for 24 h at room temperature and then dried in the air at 120 °C for 12 h before calcination in the air at 450 °C for 5 h to form  $\text{Cu}(\text{II})\text{O}$ .

**EPFR Formation.** The adsorbate chemicals, phenol (PH, Aldrich, 99+%), 2-monochlorophenol (2-MCP, Aldrich, 99+%), and 1,2-dichlorobenzene (1,2-DCBz, Sigma-Aldrich, 99% HPLC grade) were used as received without further purification.

EPFRs were formed by exposing  $\text{CuO}$ /silica particles to precursor vapors: phenol, 2-MCP, 1,2-DCBz. Prior to the precursor's exposure, the particles were heated *in situ* in the air at 450 °C for 1 h to remove organics on the surface. In addition, these particles were exposed to the selected precursor vapors at 230 °C using a custom-made vacuum exposure chamber for 5 min under vapor pressure conditions. After exposure, samples were evacuated for 1 h to remove excess nonchemisorbed adsorbate (20) at  $10^{-2}$  Torr. The dosed particles were cooled under vacuum conditions to room temperature before EPR spectra were recorded. Each experiment was repeated 3X, and the results were reproducible within radial deviation of <5%.

**EPR Analysis.** EPR spectra were recorded in a Suprasil EPR tube at room temperature using a computer-controlled Bruker EMX 10/2.7 EPR spectrometer. Instrument parameters were as follows: center field, 3470 G; sweep width, 100 G; microwave frequency, 9.7 GHz; microwave power, 2.0 mW; modulation frequency, 4.0 G; modulation amplitude, 4.0 G; receiver gain,  $3.54 \times 10^4$ ; time constant, 41.0 ms; and three scans. Radical concentration was calculated using the DPPH standard due to the similarity between the spectral profiles of DPPH and the radicals formed on  $\text{CuO}$ /silica.

**Lifetime Analysis.** The kinetic studies were performed to determine the persistency and stability of the radicals in the air. The samples were exposed to ambient air and EPR spectra obtained regularly to determine the concentration of radicals as a function of time until the sample had decayed and acquisition of the EPR spectra was at the noise level of the instrument. The  $1/e$  lifetimes ( $t_{1/e}$ ) of EPFRs were evaluated using the following mathematical expression for the first-order decay:

$$\ln(R/R_0) = kt \text{ and } t_{1/e} = 1/k$$

Rate constant  $k$  was found from the slope of the correlation between logarithm of radical concentration change ( $R/R_0$ ) vs time, and  $1/e$  lifetime was calculated.

## RESULTS AND DISCUSSION

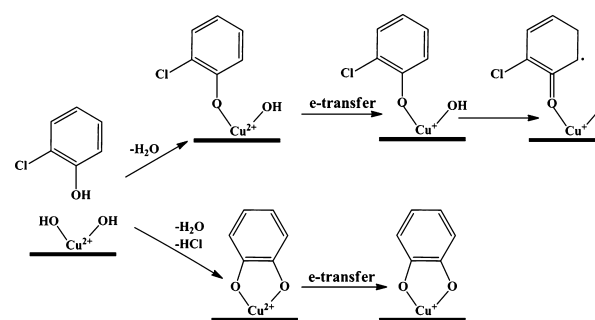
**EPFR Formation.** Adsorption of aromatic precursors on  $\text{CuO}$  supported on silica resulted in the appearance of an EPR signal centered at  $\sim 3400$  G with a narrow line width  $\Delta H_{\text{p-p}} \sim 5\text{--}7$  G for phenol and 2-MCP, and a broader line width  $\Delta H_{\text{p-p}} \sim 8\text{--}16$  G of 1,2-DCBz. Table 1 displays the spectral parameters of each adsorbate. These paramagnetic signals arise due to the interaction between the hydroxyl- and chlorine-substituted molecules with a metal oxide surface. The general mechanism of EPFR formation has been established and confirmed by our previous studies of copper, iron, nickel, zinc oxides, titania, and alumina.<sup>20,29,31,38</sup> The molecular precursors react with the surface-hydroxyl groups and chemisorbs via elimination of  $\text{H}_2\text{O}/\text{HCl}$ , resulting in a surface-bound EPFR. This interaction result in a 1-electron transfer to the metal

**Table 1.** Spectral Characteristics of EPFRs Formed on Different  $\text{CuO}$  Loading on Silica Matrix from Different Adsorbates at 230 °C

% CuO	g value			$\Delta H_{\text{p-p}}$		
	2-MCP	1,2-DCBz	PH	2-MCP	1,2-DCBz	PH
5	2.0042	2.0060	2.0039	6.7	16.0	5.2
3	2.0044	2.0057	2.0039	6.9	15.9	4.8
2	2.0039	2.0053	2.0039	5.5	15.3	5.4
1	2.0038	2.0050	2.0037	5.3	15.2	5.3
0.75	2.0040	2.0051	2.0039	5.6	14.2	5.2
0.5	2.0040	2.0048	2.0040	6.1	7.4	5.4
0.25	2.0040	2.0050	2.0038	6.0	7.7	4.6

cation center and a surface-stabilized radical. The general scheme for the reaction is presented for 2-MCP at  $\text{Cu}^{2+}$  sites on  $\text{Cu}(\text{II})\text{O}$ /silica particle surface (cf. Scheme 1).

**Scheme 1.** General Mechanism of EPFR Formation from 2-Monochlorophenol at  $\text{Cu}^{2+}$  Sites on a  $\text{CuO}$ /Silica Particle



**Radical Speciation.** The precursor–metal oxide interaction may result in more than one type of EPFR depending on the number and position of the substituent in the aromatic precursor<sup>20</sup> with the overall EPR spectrum being a superposition of those species.<sup>28–31</sup> Deconvolution of the complex EPFRs' spectra facilitated the identification of three paramagnetic species, namely, F-center, superimposed at 1.9970–2.0020, g2 (attributed to phenoxyl radicals) superimposed at 2.0035–2.0040, and g3 (attributed to semiquinone radicals) superimposed at <2.0050.<sup>29,31</sup> Depending on the relative concentration of g2 and g3 types of radicals, an overall shift of g value of the EPR signal is observed. In the current study, the overall g values for the EPFR species for phenol and 2-MCP were similar ( $\sim 2.0037\text{--}2.0044$ ) with a shift toward the lower g values for phenol (cf. Figure 1). For phenol adsorption, the

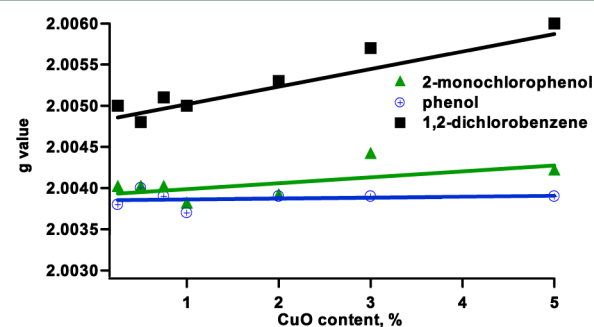


**Figure 1.** Overall g value of radical signal with changing  $\text{CuO}$  content in particles.

resultant radical signals did not change either the position or the line width with respect to concentration of copper oxide on silica (cf. Figures 1 and 2, Table 1). Thus, it is evident that no

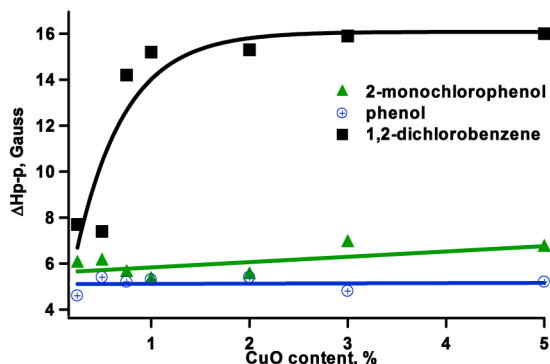


Figure 2. Change of  $\Delta H_{p-p}$  of EPR spectra with changing CuO content.

change of radical speciation occurred with decreasing CuO content. On the basis of the spectral parameters from previous studies of silica supported with 5% CuO,  $\text{Fe}_2\text{O}_3$ , and NiO, together with the current results, it can be concluded that a phenoxyl-type radical is formed on the surface of all copper concentrations<sup>20,29,31,39</sup>

For the adsorption of 2-MCP, the overall  $g$  value of spectra for all CuO concentrations changed only slightly with copper content and is within the range of 2.0038–2.0044. On the basis of the above finding, we conclude that the majority of radicals are of the chlorophenoxyl type.<sup>18</sup> On the other hand, the overall peak width,  $\Delta H_{p-p}$ , was larger on average by 1 gauss for the radical species, resulting from adsorption of 2-MCP compared with phenol adsorption (cf. Table 1) at higher CuO concentrations. This indicates the contribution of another radical species in the spectrum of 2-MCP exposed samples, and it is believed to originate from semiquinone-type radicals that are formed by the interaction between chlorine and hydroxyl groups with the surface (cf. Scheme 1). This is similar to the results obtained from other metal oxides.<sup>20,29,31,40</sup> Interestingly, unlike in the case of phenol, the peak width broadens with an increase in  $g$  value (*vide infra*).

1,2-Dichlorobenzene chemisorption on copper oxide-containing particles resulted in highly asymmetric EPR spectra and higher  $g$  values ( $>2.0048$ ) and larger line width ( $\sim 7.7$ – $16$  G) than those resulting from the adsorption of phenol and 2-MCP (cf. Figures 1 and 2 and Table 1). A high contribution of the *o*-semiquinone radicals to the overall spectrum is anticipated for 1,2-DCBz as it had been observed in other metals. Indeed, 1,2-DCBz adsorption has been reported to proceed with simultaneous displacement of both chlorine atoms, resulting in the formation of predominantly *o*-semiquinone radicals.<sup>41</sup> However, a distinct spectral change can be seen with decreasing copper content (cf. Figure 3) when the overall  $g$  values of the spectra are decreasing (cf. Figure 1). Observed dramatic spectral changes result from changing speciation of the formed radicals from predominantly semiquinone species to a more balanced ratio of chlorophenoxyl to *o*-semiquinone radicals or even predominantly chlorophenoxyl species for 0.25 and 0.5% CuO. Decreasing spectral width also supports this conclusion (cf. Figure 2). For 0.5% CuO, adsorption of 1,2-dichlorobenzene produces a spectrum that resembles more the spectrum that results from adsorption of 2-monochlorophenol

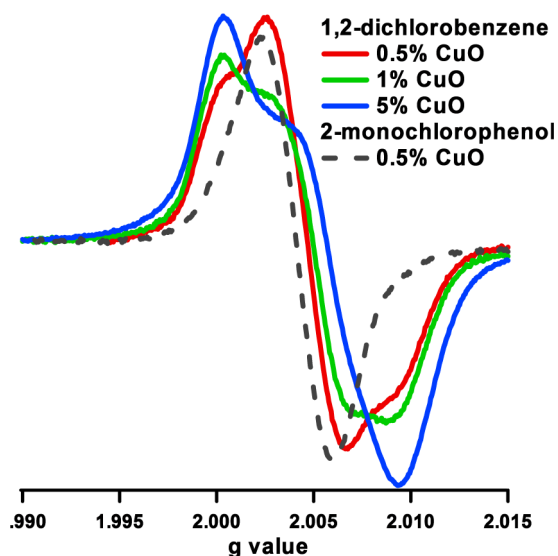


Figure 3. EPR spectra from the adsorption of 1,2-dichlorobenzene and 2-monochlorophenol on the particles containing different copper oxide concentrations.

than the one that results from higher concentrations of CuO exposed to 1,2-dichlorobenzene (cf. Figure 3).

**Surface Radical Density.** The surface concentration of radicals formed upon the adsorption of precursors on CuO/silica samples depends on the concentration of copper oxide (cf. Figures 4 and 5). In general, the adsorption of 2-MCP

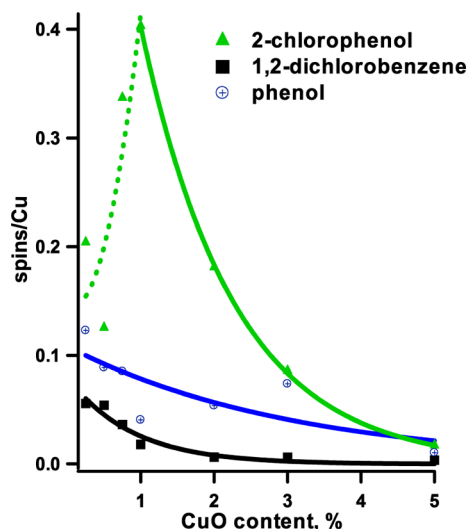
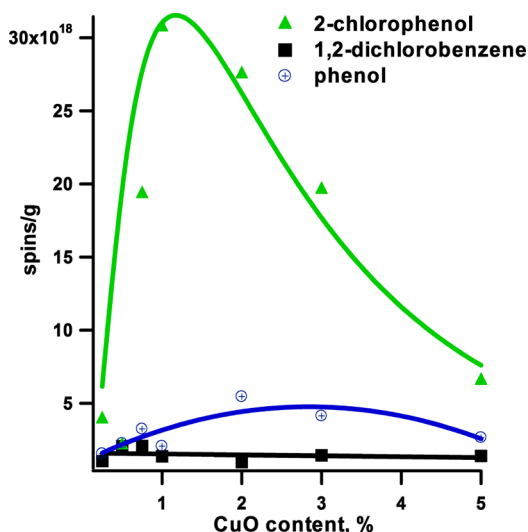


Figure 4. Dependence of EPFR density with metal concentration dosed with 1,2-Dichlorobenzene, 2-monochlorophenol, and phenol on various CuO loadings on silica.

resulted in the highest concentration of radicals on the surface, with the maximum yield at  $\sim 1\%$  CuO content. Above that concentration, the yield drops rapidly (cf. Figure 5). Chemisorption of 2-MCP occurs 11 times faster than that of a DCBz.<sup>41</sup> This is expected since chemisorption of 2-MCP requires scission of the phenolic O–H bond, which has a bond dissociation energy of 82 kcal/mol<sup>42</sup> compared with 97 kcal/mol for the C–Cl bond dissociation in 1,2-DCBz.<sup>43</sup>

Since only copper sites are active in the formation of radicals, a linear correlation between the radical yield and copper



**Figure 5.** Concentrations of organic EPFR adsorbed at 230 °C for different CuO contents based on a sample mass basis.

content should be expected. However, as presented in Figure 4, this is not the case. Data presented in Figure 4 have been fitted to exponential decrease expression (solid lines). An exponential decrease in radical density per copper atom was observed between 1% and 5% CuO content for 2-MCP adsorption, with radical density drop-off below 1%. For copper oxide content below 1%, an exponential increase of radical concentration described the observed trend the best, as marked by the dotted line in Figure 4. At the maximum observed radical concentration, one radical is formed for every ~two copper atoms in the samples. One can imagine that once an adsorbed radical occupies a copper site, the surface access to neighboring sites is hindered. Thus, we can assume a complete saturation of the surface sites with adsorbates for 1% CuO. The 1:2 ratio of EPFRs to copper (for 1% CuO loading) is an indication that all copper atoms are surface available in this case. Up to 1% CuO content CuO clusters are two-dimensional with all copper atoms to be surface available. Increasing CuO content above 1% results in three-dimensional growths of the clusters and entrapment of some of the copper atoms inside the clusters. We speculate that this is the main reason for the radical yield drop for CuO content above 1%, while the ratio of radicals to surface copper atoms (radical density) remains unchanged. Below 1% CuO content, a drop of radical density from the 2-MCP precursor can be observed (cf. Figure 4). We speculate that all copper sites are surface available at the 1% CuO content, and a further decrease in copper oxide concentration results in even smaller CuO clusters limiting the number of adsorbed species due to steric effects. At 1% CuO loading, for every 10 copper atoms, four are associated with radicals (cf. Figure 4). Assuming the decrease of cluster size with decreasing CuO content, below 1% of CuO, the clusters become smaller, limiting the number of adsorbed species (for example, a nine Cu atom flat CuO cluster could fit only three radicals—a 0.3 coverage ratio etc.). At present, we consider steric effects as a major cause of the radical yield decrease below 1% CuO content; however, electronic effects such as a lack of stabilization of reduced copper cannot be ruled out.

Phenol adsorption over CuO-containing particles resulted in both lower EPFR yield and lower radical density, when compared with 2-monochlorophenol (cf. Figures 4 and 5). In

this case, a maximum yield of radicals is detected between 2 and 3% CuO content. The differences in the radical yield of 2-monochlorophenol and phenol result from the effect of the *ortho* group substituent,<sup>29,31</sup> *ortho*-substituted aromatics being more reactive. Thus, the surface radical density increases exponentially with decreasing copper oxide content. An increase in radical density below 1% copper oxide content indicates a higher reactivity of small clusters.

The same conclusion is supported by an exponential decrease in radical density with increasing copper oxide content after 1,2-dichlorobenzene adsorption (cf. Figure 4). As discussed earlier, by decreasing the copper oxide content, radical species are gradually changing from bidentate semiquinone to monodentate phenoxyl radicals. This results in a “more closely” packed species on the surface. Indeed, the adsorption of 1,2-dichlorobenzene is the only case where a small linear increase of EPFR yield is detected with decreasing copper oxide content (cf. Figure 5).

**EPFRs Persistency.** One of the most important characteristics of EPFRs from an environmental perspective is their persistency in the environment. EPFRs have been reported to have a much longer lifetime compared with other radicals such as acyl, hydroxyl, or superoxide,<sup>44,45</sup> which makes them environmentally hazardous when emitted from combustion sources. As previously mentioned, particulate matter may contain a varying concentration of metal oxides; therefore decay times have to be evaluated relative to the metal concentration. The EPFR 1/*e* lifetime in ambient air which is associated with CuO is depicted in Figure 6. It is evident that

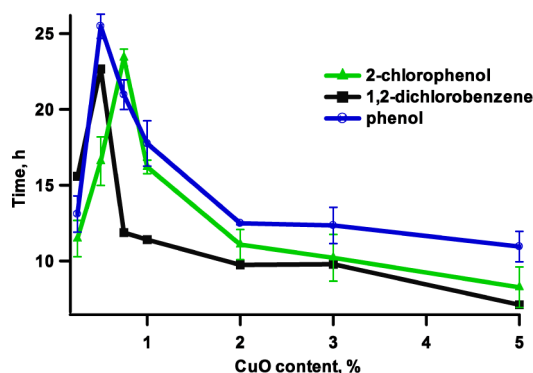


**Figure 6.** EPFRs 1/*e* lifetimes in ambient air at room temperature formed on different CuO loadings on silica at 230 °C.

by decreasing the copper oxide content, EPFRs 1/*e* lifetimes increase to the maximum value at ~0.5–0.75% CuO. Interestingly, for 1,2-dichlorobenzene and 2-monochlorophenol precursors, their observed maximum 1/*e* lifetimes are very similar (22–23 h), indicating again similar species dominating the surface at CuO content—chlorophenoxyl species. At higher copper oxide contents, a difference between 1/*e* lifetimes of those two samples is notable. This is in line with the previous studies that demonstrated longer lifetimes of phenoxyl compared with a semiquinone-type radical. It is also worth it to note that small clusters do not stabilize radicals as efficiently as indicated by the drop in the lifetime of EPFRs below 0.5% concentration. A word of caution is therefore necessary: ~0.5% CuO should not be taken as a limit for the highest stability of radicals in environmental samples. In real life, a cluster size distribution may not correlate with the concentration as in the case of those synthetic samples.



In summary, our results indicate that the reactivity of aromatic compounds on particulates is dependent on the concentrations of CuO. The result of the interaction with the surfaces produces EPFRs that are stable and persist for hours. Though we could not prove it directly, it is inferred that the differences in reactivity result from different cluster sizes of copper oxide affecting concentration, persistency, and speciation of EPFRs. The smaller the size of the nanoclusters, the higher is the ability to catalyze EPFRs' formation/stabilization. Changing the persistency of EPFRs with different CuO concentrations is only partially correlated with changing radical speciation and indicates the role of cluster size in radical stabilization. The consequence of the higher stability of EPFRs on smaller clusters is transport to long distances from the source. Another potential implication of the presented studies is the potential of engineered nanomaterials in consumer products to amplify EPFRs production.

## AUTHOR INFORMATION

### Corresponding Author

\*E-mail: slomni1@lsu.edu.

### Notes

The authors declare no competing financial interest.

## ACKNOWLEDGMENTS

This study was supported by National Institute of Environmental Health Sciences, Superfund Research Program grant # 2 P-42 ES013648

## REFERENCES

- (1) Hamade, A. K.; Rabold, R.; Tankersley, C. G. Adverse cardiovascular effects with acute particulate matter and ozone exposures: interstrain variation in mice. *Environ. Health Perspect.* **2008**, *116*, 1033.
- (2) Li, N.; Xia, T.; Nel, A. E. The role of oxidative stress in ambient particulate matter-induced lung diseases and its implications in the toxicity of engineered nanoparticles. *Free Radical Biol. Med.* **2008**, *44*, 1689–99.
- (3) Kang, Y. J.; Li, Y.; Zhou, Z.; Roberts, A.; Cai, L.; et al. Elevation of serum endothelins and cardiotoxicity induced by particulate matter (PM<sub>2.5</sub>) in rats with acute myocardial infarction. *Cardiovasc. Toxicol.* **2002**, *2*, 253–61.
- (4) Danielsen, P. H.; Möller, P.; Jensen, K. A.; Sharma, A. K.; Wallin, H. K.; et al. Oxidative Stress, DNA Damage, and Inflammation Induced by Ambient Air and Wood Smoke Particulate Matter in Human A549 and THP-1 Cell Lines. *Chem. Res. Toxicol.* **2011**, *24*, 168–84.
- (5) Risom, L.; Möller, P.; Loft, S. Oxidative stress-induced DNA damage by particulate air pollution. *Mutat. Res., Fundam. Mol. Mech. Mutagen.* **2005**, *592*, 119–37.
- (6) de Kok, T. M.; Hogervorst, J. G.; Briedé, J. J.; van Herwijnen, M. H.; Maas, L. M.; et al. Genotoxicity and physicochemical characteristics of traffic-related ambient particulate matter. *Environ. Mol. Mutagen.* **2005**, *46*, 71–80.
- (7) Dellinger, B.; Pryor, W. A.; Cueto, R.; Squadrito, G. L.; Hegde, V.; Deutsch, W. A. Role of Free Radicals in the Toxicity of Airborne Fine Particulate Matter. *Chem. Res. Toxicol.* **2001**, *14*, 1371–7.
- (8) Prahalad, A. K.; Inmon, J.; Dailey, L. A.; Madden, M. C.; Ghio, A. J.; Gallagher, J. E. Air Pollution Particles Mediated Oxidative DNA Base Damage in a Cell Free System and in Human Airway Epithelial Cells in Relation to Particulate Metal Content and Bioreactivity. *Chem. Res. Toxicol.* **2001**, *14*, 879–87.
- (9) Nel, A. E.; Diaz-Sanchez, D.; Li, N. The role of particulate pollutants in pulmonary inflammation and asthma: evidence for the involvement of organic chemicals and oxidative stress. *Curr. Opin. Pulm. Med.* **2001**, *7*, 20–6.
- (10) Peters, A.; Dockery, D. W.; Muller, J. E.; Mittleman, M. A. Increased particulate air pollution and the triggering of myocardial infarction. *Circulation* **2001**, *103*, 2810–5.
- (11) *Understanding the Health Effects of Ambient Ultrafine Particles*; Particles HEIRPoU, Institute HE, Health Effects Institute: Boston, MA, 2013.
- (12) Li, N.; Sioutas, C.; Cho, A.; Schmitz, D.; Misra, C.; et al. Ultrafine particulate pollutants induce oxidative stress and mitochondrial damage. *Environ. Health Perspect.* **2003**, *111*, 455.
- (13) Brown, D. M.; Wilson, M. R.; MacNee, W.; Stone, V.; Donaldson, K. Size-dependent proinflammatory effects of ultrafine polystyrene particles: a role for surface area and oxidative stress in the enhanced activity of ultrafines. *Toxicol. Appl. Pharmacol.* **2001**, *175*, 191–9.
- (14) Valavanidis, A.; Fiotakis, K.; Vlachogianni, T. Airborne particulate matter and human health: toxicological assessment and importance of size and composition of particles for oxidative damage and carcinogenic mechanisms. *J. Environ. Sci. Health, Part C: Environ. Carcinog. Ecotoxicol. Rev.* **2008**, *26*, 339–62.
- (15) Franck, U.; Herbarth, O.; Röder, S.; Schlink, U.; Borte, M.; et al. Respiratory effects of indoor particles in young children are size dependent. *Sci. Total Environ.* **2011**, *409*, 1621–31.
- (16) Khachatryan, L.; Vejerano, E.; Lomnicki, S.; Dellinger, B. Environmentally Persistent Free Radicals (EPFRs). 1. Generation of Reactive Oxygen Species in Aqueous Solutions. *Environ. Sci. Technol.* **2011**, *45*, 8559–66.
- (17) Dellinger, B.; Khachatryan, L.; Masko, S.; Lomnicki, S. Free Radicals in Tobacco Smoke. *Mini-Rev. Org. Chem.* **2011**, *8*, 427–33.
- (18) Lomnicki, S.; Dellinger, B. A Detailed Mechanism of the Surface-Mediated Formation of PCDD/F from the Oxidation of 2-Chlorophenol on a CuO/Silica Surface. *J. Phys. Chem. A* **2003**, *107*, 4387–95.
- (19) Cormier, S. A.; Lomnicki, S.; Backes, W.; Dellinger, B. Origin and health impacts of emissions of toxic by-products and fine particles from combustion and thermal treatment of hazardous wastes and materials. *Environ. Health Perspect.* **2006**, *114*, 810.
- (20) Lomnicki, S.; Truong, H.; Vejerano, E.; Dellinger, B. Copper Oxide-Based Model of Persistent Free Radical Formation on Combustion-Derived Particulate Matter. *Environ. Sci. Technol.* **2008**, *42*, 4982–8.
- (21) Dellinger, B.; Lomnicki, S.; Khachatryan, L.; Maskos, Z.; Hall, R. W.; et al. Formation and stabilization of persistent free radicals. *Proc. Combust. Inst.* **2007**, *31*, S21–8.
- (22) Allouis, C.; Beretta, F.; D'Alessio, A. Structure of inorganic and carbonaceous particles emitted from heavy oil combustion. *Chemosphere* **2003**, *51*, 1091–6.
- (23) Bell, M. L.; Ebisu, K.; Peng, R. D.; Samet, J. M.; Dominici, F. Hospital admissions and chemical composition of fine particle air pollution. *Am. J. Respir. Crit. Care Med.* **2009**, *179*, 1115.
- (24) Peng, R. D.; Bell, M. L.; Geyh, A. S.; McDermott, A.; Zeger, S. L.; et al. Emergency admissions for cardiovascular and respiratory diseases and the chemical composition of fine particle air pollution. *Environ. Health Perspect.* **2009**, *117*, 957.
- (25) Dominici, F.; Peng, R. D.; Ebisu, K.; Zeger, S. L.; Samet, J. M.; Bell, M. L. Does the effect of PM<sub>10</sub> on mortality depend on PM nickel and vanadium content? A reanalysis of the NMMAPS data. *Environ. Health Perspect.* **2007**, *115*, 1701.
- (26) Dreher, K. L.; Jaskot, R. H.; Lehmann, J. R.; Richards, J. H.; Ghio, J. K. M. A. J.; Costa, D. L. Soluble transition metals mediate residual oil fly ash induced acute lung injury. *J. Toxicol. Environ. Health, Part A* **1997**, *50*, 285–305.
- (27) Karamanov, A.; Pelino, M.; Salvo, M.; Metekovits, I. Sintered glass-ceramics from incinerator fly ashes. Part II. The influence of the particle size and heat-treatment on the properties. *J. Eur. Ceram. Soc.* **2003**, *23*, 1609–15.
- (28) Lomnicki, S.; Truong, H.; Vajereno, E.; Dellinger, B. Copper Oxide-Based Model of Persistent Free Radical Formation on Combustion Derived Particulate Matter. *Environ. Sci. Technol.* **2008**, *42*, 4982–8.

- (29) Vejerano, E.; Lomnicki, S.; Dellinger, B. Formation and Stabilization of Combustion-Generated Environmentally Persistent Free Radicals on an Fe(III)2O3/Silica Surface. *Environ. Sci. Technol.* **2010**, *45*, 589–94.
- (30) Vejerano, E.; Lomnicki, S.; Dellinger, B. Lifetime of combustion-generated environmentally persistent free radicals on Zn(ii)O and other transition metal oxides. *J. Environ. Monit.* **2012**, *14*, 2803–6.
- (31) Vejerano, E.; Lomnicki, S. M.; Dellinger, B. Formation and Stabilization of Combustion-Generated, Environmentally Persistent Radicals on Ni(II)O Supported on a Silica Surface. *Environ. Sci. Technol.* **2012**, *46*, 9406–11.
- (32) Zhou, X.; Xu, W.; Liu, G.; Panda, D.; Chen, P. Size-Dependent Catalytic Activity and Dynamics of Gold Nanoparticles at the Single-Molecule Level. *J. Am. Chem. Soc.* **2009**, *132*, 138–46.
- (33) Wilson, O. M.; Knecht, M. R.; Garcia-Martinez, J. C.; Crooks, R. M. Effect of Pd nanoparticle size on the catalytic hydrogenation of allyl alcohol. *J. Am. Chem. Soc.* **2006**, *128*, 4510–1.
- (34) Bezemer, G. L.; Bitter, J. H.; Kuipers, H. P. C. E.; Oosterbeek, H.; Holewijn, J. E.; et al. Cobalt Particle Size Effects in the Fischer–Tropsch Reaction Studied with Carbon Nanofiber Supported Catalysts. *J. Am. Chem. Soc.* **2006**, *128*, 3956–64.
- (35) Grass, M.; Rioux, R.; Somorjai, G. Dependence of Gas-Phase Crotonaldehyde Hydrogenation Selectivity and Activity on the Size of Pt Nanoparticles (1.7–7.1 nm) Supported on SBA-15. *Catal. Lett.* **2009**, *128*, 1–8.
- (36) Doyle, A. M.; Shaikhutdinov, S. K.; Freund, H.-J. Surface-Bonded Precursor Determines Particle Size Effects for Alkene Hydrogenation on Palladium. *Angew. Chem., Int. Ed.* **2005**, *44*, 629–31.
- (37) Burda, C.; Chen, X.; Narayanan, R.; El-Sayed, M. A. Chemistry and Properties of Nanocrystals of Different Shapes. *Chem. Rev.* **2005**, *105*, 1025–102.
- (38) Patterson, M. C.; Keilbart, N. D.; Kiruri, L. W.; Thibodeaux, C. A.; Lomnicki, S.; et al. EPFR formation from phenol adsorption on Al2O3 and TiO2: EPR and EELS studies. *Chem. Phys.* **2013**, *422*, 277–82.
- (39) Boyd, S. A.; Mortland, M. M. Dioxin radical formation and polymerization on Cu(II)-smectite. *Nature* **1985**, *316*, 532–5.
- (40) Patterson M. C., Keilbart N. D., Kiruri L. W., Thibodeaux C. A., Lomnicki S., et al. EPFR formation from phenol adsorption on Al2O3 and TiO2: EPR and EELS studies. *Chem. Phys.*
- (41) Alderman, S. L.; Farquar, G. R.; Poliakoff, E. D.; Dellinger, B. An Infrared and X-ray Spectroscopic Study of the Reactions of 2-Chlorophenol, 1,2-Dichlorobenzene, and Chlorobenzene with Model CuO/Silica Fly Ash Surfaces. *Environ. Sci. Technol.* **2005**, *39*, 7396–401.
- (42) Khachatryan, L.; Asatryan, R.; Dellinger, B. Development of expanded and core kinetic models for the gas phase formation of dioxins from chlorinated phenols. *Chemosphere* **2003**, *52*, 695–708.
- (43) Tsang, W. Mechanisms for the Formation and Destruction of Chlorinated Organic Products of Incomplete Combustion. *Combust. Sci. Technol.* **1990**, *74*, 99–116.
- (44) Pryor, W. A. Oxy-Radicals and Related Species: Their Formation, Lifetimes, and Reactions. *Annu. Rev. Physiol.* **1986**, *48*, 657–67.
- (45) Finkelstein, E.; Rosen, G. M.; Rauckman, E. J. Production of hydroxyl radical by decomposition of superoxide spin-trapped adducts. *Mol. Pharmacol.* **1982**, *21*, 262–5.